# Supporting Information

# Structural Insights into the Mechanism of High Affinity Binding of Ochratoxin A by a DNA Aptamer

Guohua Xu[1], Jiajing Zhao[1, 5], Hao Yu[2, 4], Chen Wang[1, 4], Yangyu Huang[6], Qiang Zhao[2, 3, 4, *], Xin Zhou[1], Conggang Li[1, *] and Maili Liu[1]

[1] Key Laboratory of Magnetic Resonance in Biological Systems, State Key Laboratory of Magnetic Resonance and Atomic and Molecular Physics, National Center for Magnetic Resonance in Wuhan, Wuhan National Laboratory for Optoelectronics, Wuhan Institute of Physics and Mathematics, Innovation Academy for Precision Measurement Science and Technology, Chinese Academy of Sciences, Wuhan, 430071, P. R. China.

[2] State Key Laboratory of Environmental Chemistry and Ecotoxicology, Research Center for Eco-Environmental Sciences, Chinese Academy of Sciences, Beijing, 100085, P. R. China.

[3] Hangzhou Institute for Advanced Study, UCAS, Hangzhou, 310000, P. R. China.

[4] University of Chinese Academy of Sciences, Beijing, 100049, P.R. China.

[5] Xi'an Modern Chemistry Research Institute, Xi'an, 710065, P.R. China.

[6] Shaoyang University, Shaoyang, 422000, P.R. China.

* To whom correspondence should be addressed. Email: conggangli@wipm.ac.cn (Conggang Li) qiangzhao@rcees.ac.cn (Qiang Zhao)

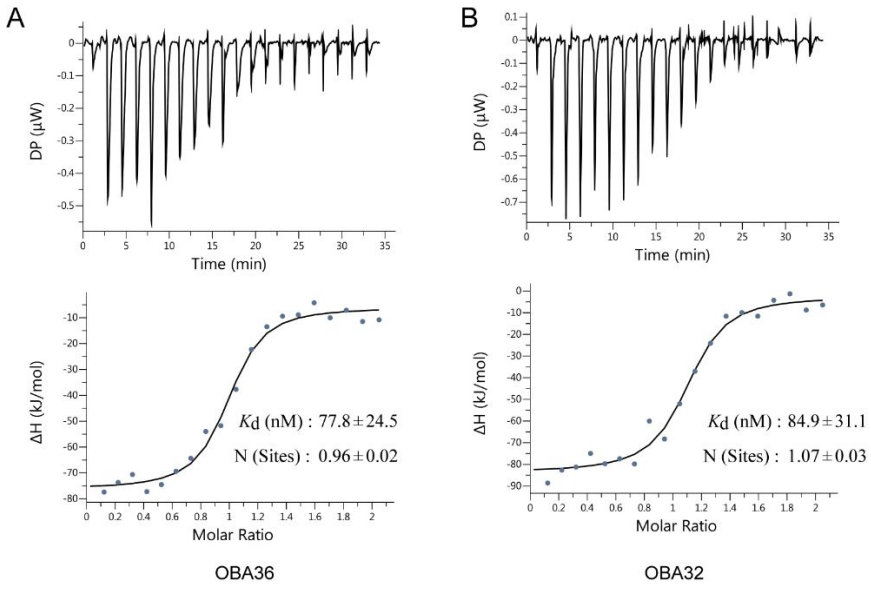


**Figure S1**. ITC titration curves for the binding of aptamer and OTA. The $K_d$ value closely corresponds to that measured using FP (Fluorescence Polarization).

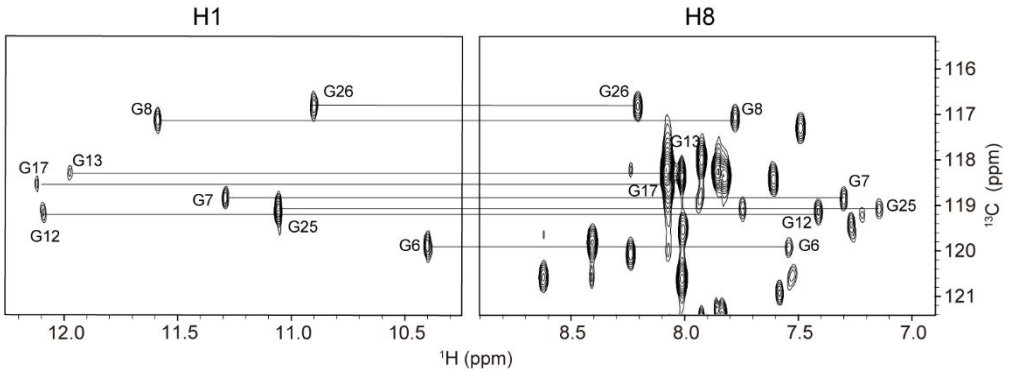


**Figure S2**. Heteronuclear multi-bond correlations (HMBC) spectrum of OBA32-OTA complex at natural abundance at 298 K, showing H1 and H8 proton assignments by through-bond correlations between imino and H8 protons via $^{13}$C5.

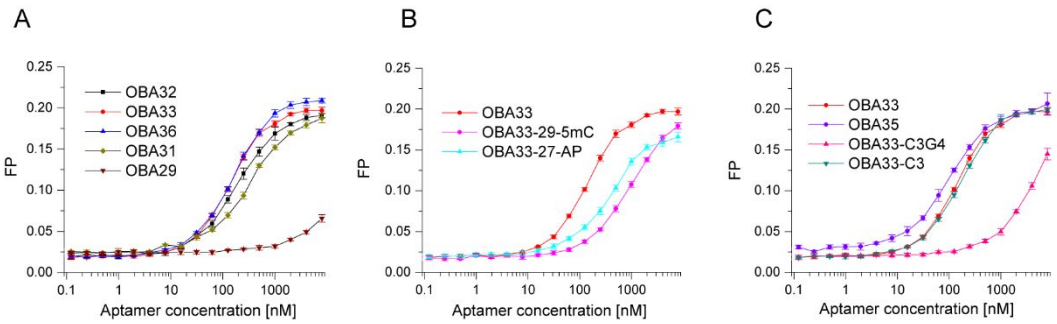


**Figure S3**. Fluorescence polarization titration of OTA with OBA aptamers.

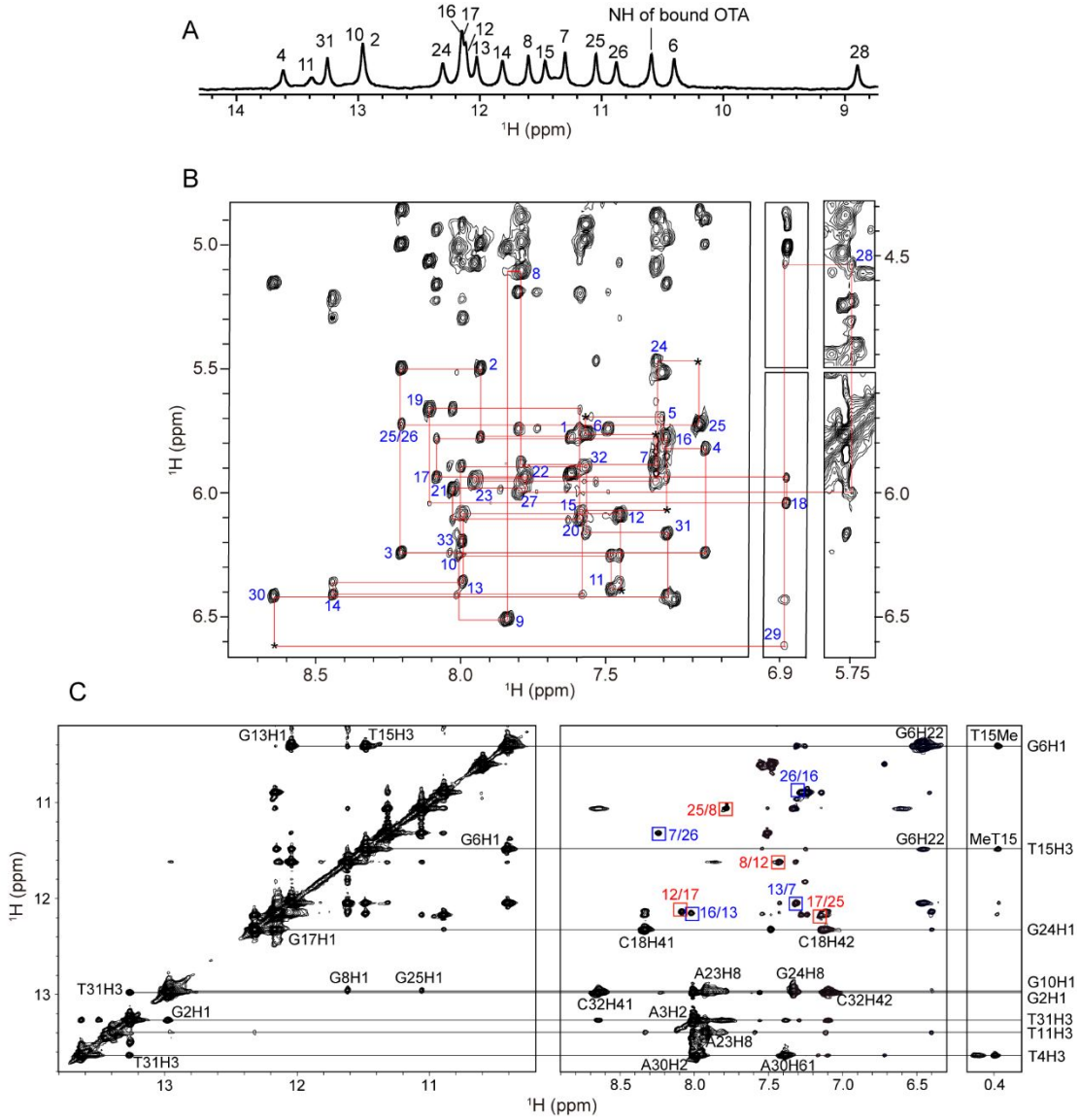


**Figure S4**. Assignments of OBA33-OTA complex. (A) Imino proton spectra of OBA33-OTA complex. (B) NOESY spectrum (mixing time, 500 ms) of OBA33-OTA complex in $D_2O$ buffer at 308 K, showing the H8/6-H1′ sequential connectivities. Intraresidue H8/6-H1′ cross-peaks are labeled with residue numbers. Missing connectivities are marked with asterisks. (C) Expanded NOESY spectrum (mixing time, 300 ms) of OBA33-OTA complex in $H_2O$ buffer at 288 K, correlating NOEs between imino protons and amino/base protons. The arrangements of G-tetrads were identified from framed cross-peaks with the residue number of imino protons labeled in the first position and that of H8 protons in the second position.

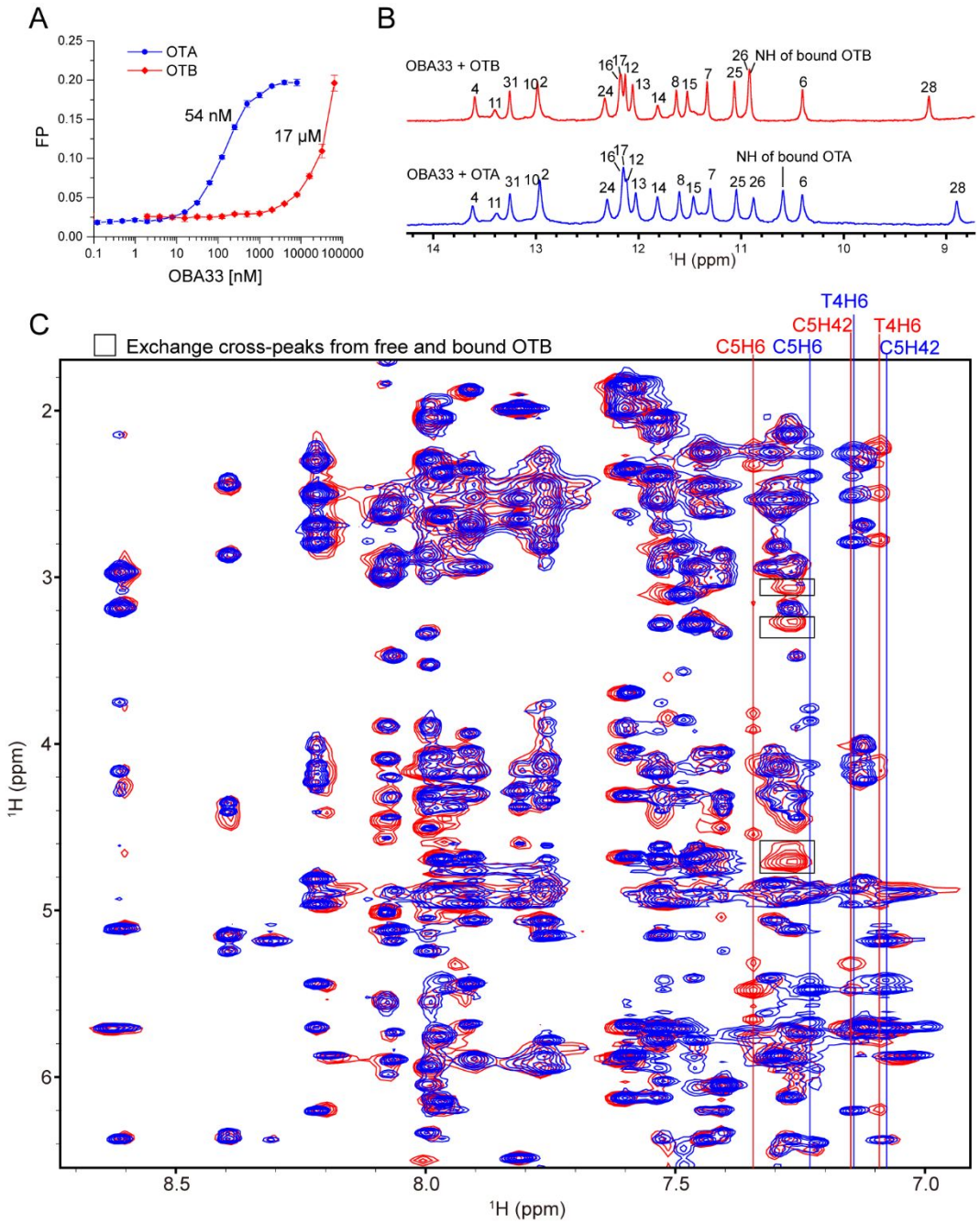


**Figure S5**. Fluorescence polarization titration of OTA or OTB with OBA33 aptamers (A). 1D $^{1}$H (B) and 2D NOESY (C) NMR spectra of OBA33 in the presence of OTA (blue) or OTB (red) in phosphate salt solution containing 10 mM $Mg^{2+}$ at 288 K.

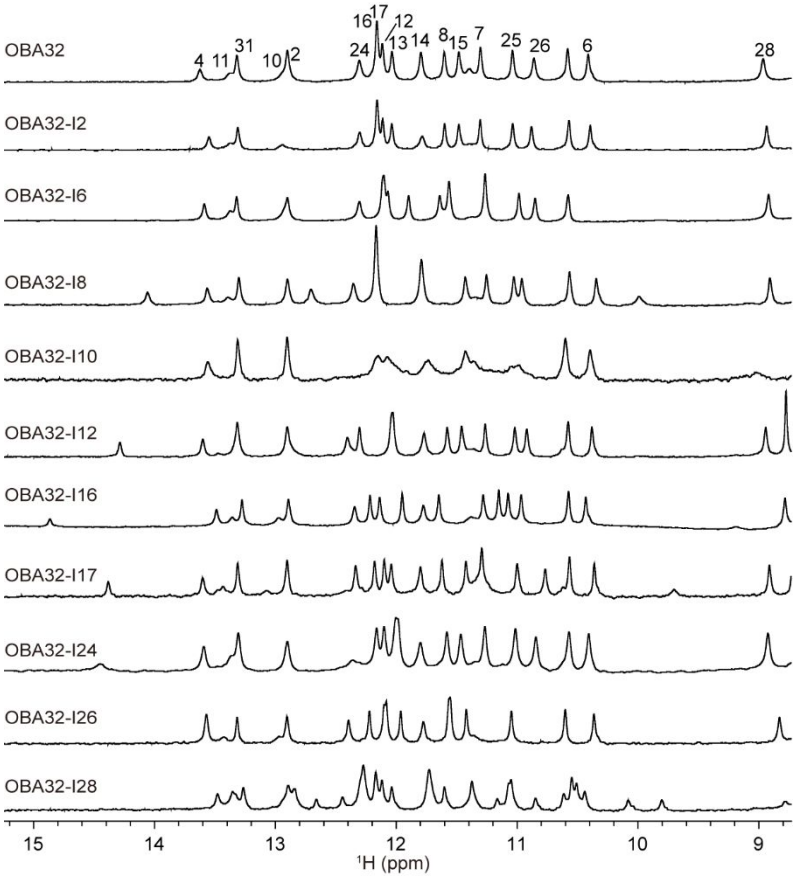


**Figure S6**. Imino regions of $^{1}$H NMR spectra of OBA32 aptamer with the replacement of G by inosole (I) in the presence of OTA.

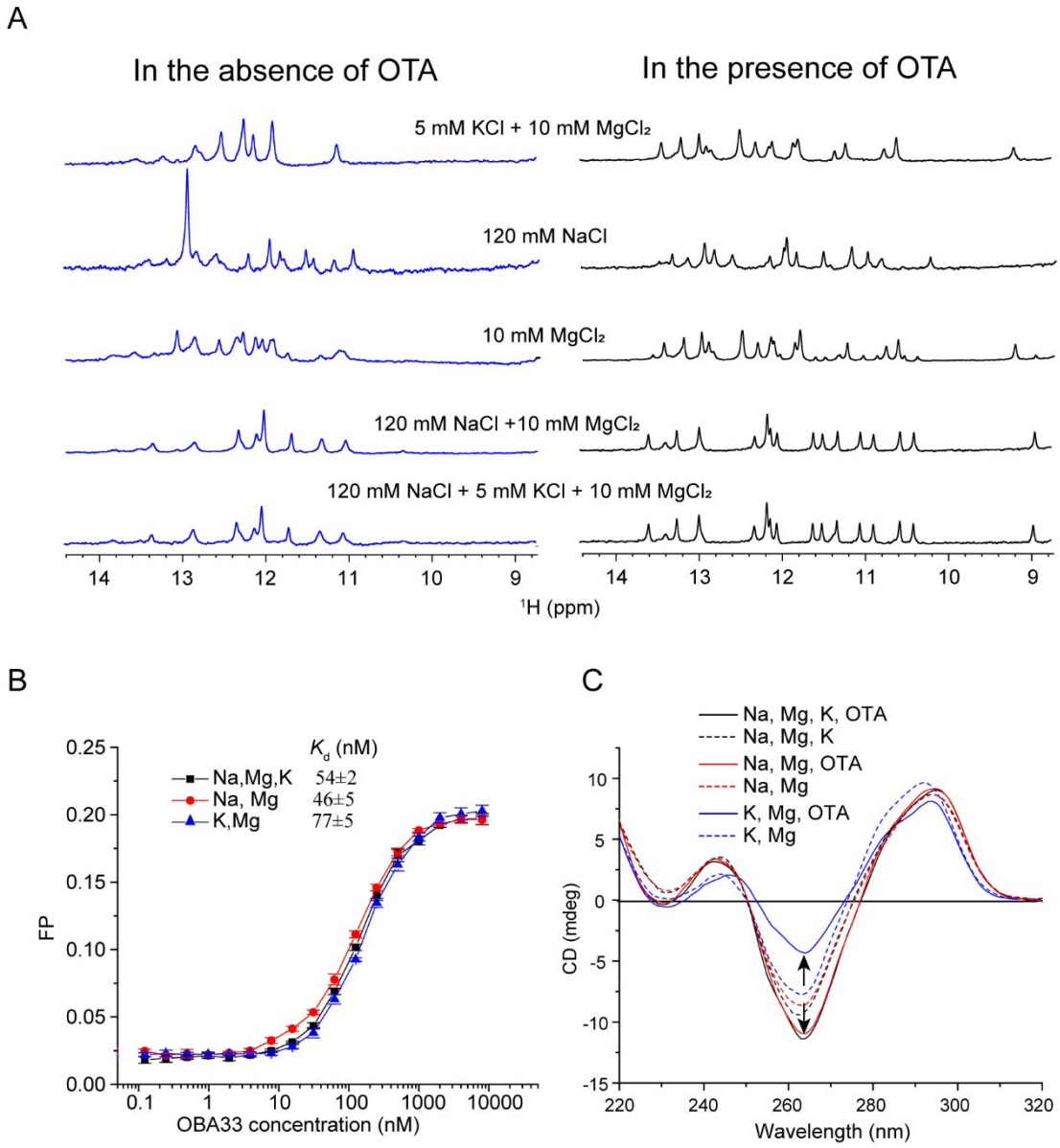


**Figure S7**.(A) Imino regions of $^{1}$H NMR spectra of OBA33 aptamer in the presence /absence of OTA in the 10 mM Tris-HCl buffer including different ions (pH 7.5) at 288 K. (B) FP titration of OTA with OBA33 aptamer in 10 mM Tris-HCl buffer including different ions (pH 7.5). (C) CD data of OBA33 aptamer (10 μM) in the presence or absence of 2 equivalents of OTA in 10 mM Tris-HCl buffer including different ions (pH 7.5). The concentration of ions in FP and CD experiments are the same as that in NMR experiments.

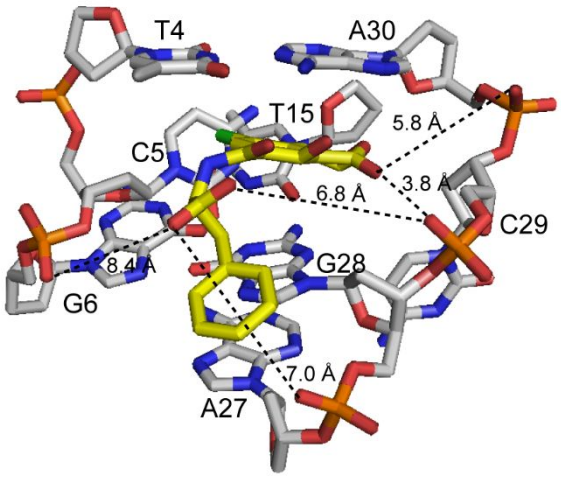


**Figure S8**. OTA Binding pocket showing that the negatively charged carboxyl and dissociated Ph-OH of OTA are close to negatively charged phosphate group of OBA33 in OBA33-OTA complex.

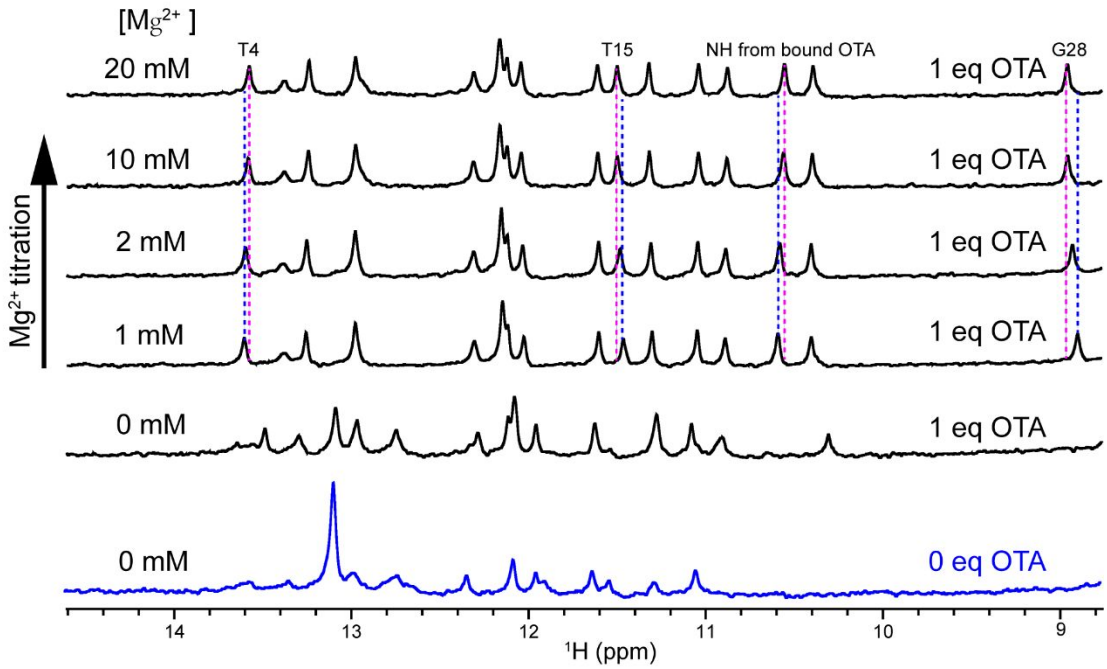


**Figure S9**. NMR titration experiment showing the effect of $Mg^{2+}$ on the imino proton region of OBA33 aptamer in the presence of 1 equivalent of OTA. NMR spectra were acquired in 10 mM Tris-HCl (pH 7.5) buffer containing 120 mM NaCl at 288 K.

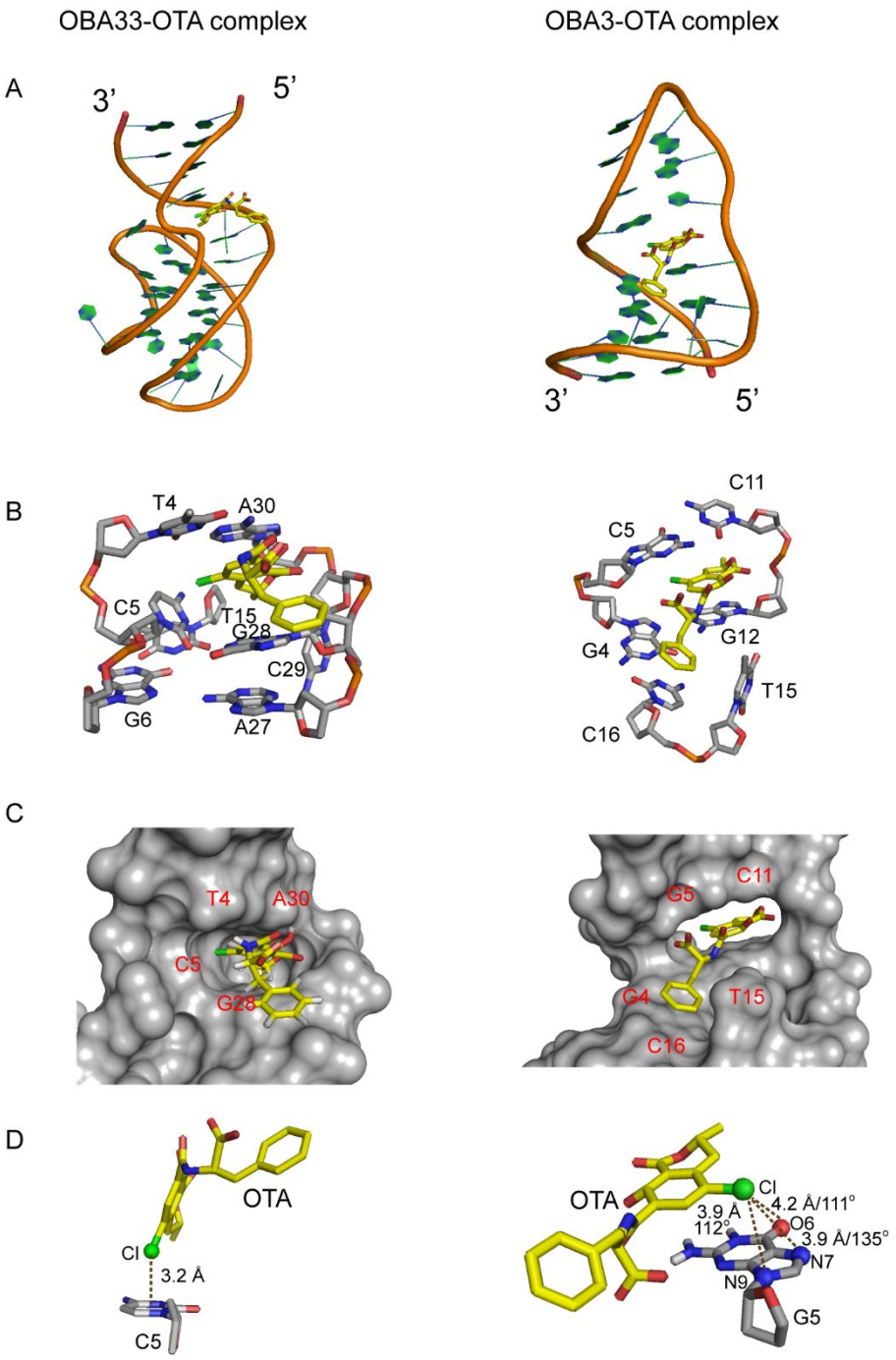


**Figure S10**. The structural comparison of OBA33-OTA (PDB code: 7W9N) and OBA3-OTA (PDB code: 6J2W) complexes. (A) Overall structures. (B) The structures of binding pockets. (C) The surface of binding pockets. (D) Halogen bonds.

**Table S1**. Sequence and dissociation constant of aptamers.

| Name | Sequence | $K_d$ (nM) |
|---|---|---|
| OBA32 | GATCGGGTGTGGGTGGCGTAAAGGGAGCATCG | 67±3 |
| OBA36 | GATCGGGTGTGGGTGGCGTAAAGGGAGCATCGGACA | 58±2 |
| OBA33 | CGATCGGGTGTGGGTGGCGTAAAGGGAGCATCG | 54±2 |
| OBA33-C3 | CGCTCGGGTGTGGGTGGCGTAAAGGGAGCAGCG | 61±2 |
| OBA35 | GCGCTCGGGTGTGGGTGGCGTAAAGGGAGCAGCGC | 35±4 |
| OBA33-29-5mC | CGATCGGGTGTGGGTGGCGTAAAGGGAG(5mC)ATCG | 472±17 |
| OBA33-27-AP | CGATCGGGTGTGGGTGGCGTAAAGGG(AP)GCATCG | 1053±48 |
| OBA33-C3G4 | CGCGCGGGTGTGGGTGGCGTAAAGGGAGCCGCG | 1736±63 |
| OBA31 | GATCGGGTGTGGGTGGCGTAAAGGGAGCATC | 141±7 |
| OBA29 | ATCGGGTGTGGGTGGCGTAAAGGGAGCAT | 11300±600 |

Binding buffer containing 10 mM Tris-HCl (pH 7.5), 10 mM $MgCl_2$, 120 mM NaCl, 5 mM KCl, and 0.1% Tween 20

**Table S2.** Proton chemical shift of OBA33-OTA complex. The chemical shift values for carbon hydrogens and active hydrogens are from NMR spectra acquired in $D_2O$ buffer at 308 K and from NMR spectra acquired in $H_2O$ buffer at 288 K, respectively.

| Residue | H1/H3 | H41/H21 /H61 | H42/H22 /H62 | H5/Me /H2 | H1' | H2' | H2'' | H3' | H4' | H5' | H5'' | H8/H6 |
|---|---|---|---|---|---|---|---|---|---|---|---|---|
| C1 | | 8.19 | 7.04 | 5.91 | 5.77 | 1.87 | 2.37 | 4.7 | 4.07 | 3.72 | 3.72 | 7.62 |
| G2 | 12.96 | | | | 5.49 | 2.70 | 2.72 | 4.99 | 4.31 | 3.97 | 4.08 | 7.93 |
| A3 | | 7.89 | 6.08 | 8.03 | 6.23 | 2.54 | 2.82 | 4.99 | 4.43 | 4.21 | 4.17 | 8.20 |
| T4 | 13.62 | | | 1.10 | 5.81 | 2.27 | 1.63 | 4.89 | 4.16 | 4.22 | 4.23 | 7.17 |
| C5 | | 5.41 | 7.08 | 5.51 | 5.69 | 1.04 | 2.39 | 4.56 | 3.16 | 3.84 | 3.90 | 7.30 |
| G6 | 10.40 | 9.92 | 6.43 | | 5.75 | 2.84 | 3.13 | 4.97 | 4.33 | 3.88 | 3.66 | 7.57 |
| G7 | 11.29 | 8.91 | 6.53 | | 5.88 | 2.89 | 2.64 | 4.88 | 4.40 | | | 7.32 |
| G8 | 11.59 | 9.98 | 6.19 | | 5.10 | 2.48 | 2.76 | 4.99 | 4.26 | 4.16 | | 7.79 |
| T9 | | | | 2.03 | 6.51 | 2.56 | 2.70 | 5.01 | 4.61 | 4.32 | 4.43 | 7.84 |
| G10 | 12.93 | | | | 6.24 | 2.94 | 2.65 | 4.78 | 4.53 | 4.20 | 4.35 | 8.00 |
| T11 | 13.36 | | | 1.15 | 6.39 | 2.29 | 2.48 | 4.7 | 3.07 | 4.10 | 4.10 | 7.47 |
| G12 | 12.1 | 9.37 | | | 6.08 | 3.38 | 2.92 | 5.07 | 4.94 | 4.54 | 4.17 | 7.44 |
| G13 | 12.01 | 9.92 | 6.72 | | 6.36 | 2.91 | 2.49 | 5.29 | 4.43 | 4.35 | 4.38 | 7.99 |
| G14 | 11.79 | | | | 6.40 | 2.49 | 2.90 | 5.20 | 4.45 | 4.40 | 4.51 | 8.43 |
| T15 | 11.45 | | | 0.44 | 6.07 | 2.18 | 2.75 | 5.01 | 4.50 | 3.67 | 3.67 | 7.58 |
| G16 | 12.12 | | | | 5.77 | 3.52 | 2.95 | 4.94 | 4.34 | 3.67 | 3.96 | 7.28 |
| G17 | 12.14 | | | | 5.93 | 2.59 | 2.90 | 5.16 | 4.48 | 4.35 | 4.35 | 8.09 |
| C18 | | 8.30 | 7.08 | 5.22 | 6.04 | 0.81 | 1.82 | 4.46 | 4.23 | 4.12 | 3.93 | 6.87 |
| G19 | | | | | 5.64 | 3.00 | 2.65 | 5.06 | 4.57 | 3.93 | 4.12 | 8.10 |
| T20 | | | | 1.86 | 6.09 | 1.97 | 2.01 | 4.39 | 4.03 | 3.92 | 3.95 | 7.58 |
| A21 | | | | 7.83 | 5.98 | 2.12 | 2.35 | 4.56 | 3.26 | 3.58 | 2.97 | 8.02 |
| A22 | | | | 7.58 | 5.93 | 2.67 | 2.48 | 4.77 | 4.20 | 3.83 | 3.84 | 7.78 |
| A23 | | | | 7.52 | 5.95 | 2.56 | 2.98 | 5.07 | 4.36 | 4.19 | 4.19 | 7.94 |
| G24 | 12.29 | | | | 5.46 | 2.28 | 2.57 | 4.87 | 4.23 | 4.06 | 4.11 | 7.33 |
| G25 | 11.03 | 8.62 | 6.57 | | 5.72 | 2.73 | 2.35 | 4.86 | 4.25 | 4.05 | 4.05 | 7.16 |
| G26 | 10.86 | 10.02 | 6.04 | | | 2.34 | 2.72 | 4.85 | 4.29 | 4.05 | 4.05 | 8.20 |
| A27 | | | | 7.25 | 5.99 | 2.54 | 2.61 | 5.18 | 4.37 | 4.13 | 3.92 | 7.79 |
| G28 | 8.89 | | | | 4.54 | 0.93 | 2.55 | 4.68 | | 3.81 | | 5.74 |
| C29 | | | | 6.43 | 6.61 | 2.01 | 2.15 | 4.24 | 4.33 | 3.81 | 3.96 | 6.87 |
| A30 | | 7.36 | 5.74 | 8.00 | 6.41 | 3.00 | 3.21 | 5.15 | 4.66 | 3.80 | 4.22 | 8.64 |
| T31 | 13.24 | | | 1.39 | 6.15 | 2.18 | 2.56 | 4.97 | 4.44 | 4.34 | 4.19 | 7.29 |
| C32 | | 8.63 | 7.07 | 5.76 | 5.88 | 2.07 | 2.43 | 4.91 | 4.19 | 4.35 | 4.35 | 7.55 |
| G33 | | | | | 6.19 | 2.66 | 2.43 | 4.72 | 4.21 | 4.12 | 4.14 | 7.99 |

**Table S3**. Statistics of the computed ten structures of OBA33-OTA complex

| | |
|---|---|
| **Distance restraints** | |
| Intraresidue | 112 |
| Sequencial | 142 |
| Long-range | 65 |
| Intermolecular | 41 |
| **Other restraints** | |
| Hydrogen bond restraints | 90 |
| Sugar pucker restraints | 60 |
| Dihedral angles | 100 |
| Repulsive | 2 |
| **NOE violations** | |
| Number (>0.2 Å) | 3 |
| RMSD of vilations (Å) | 0.043 ± 0.002 |
| Max. distance constraint violation (Å) | 0.262 |
| **Deviations from the ideal covalent geometry** | |
| Bond lengths (Å) | 0.002 ± 0.000 |
| Bond angles (deg) | 0.480 ± 0.019 |
| Impropers (deg) | 0.307 ± 0.007 |
| **Pairwise all heavy atoms RMSD values (Å)** | |
| Entire complex | 0.57 ± 0.14 |

**Table S4**. Intermolecular NOEs between OTA and OBA33 aptamer protons in OBA33-OTA complex.

| OTA protons | OBA33 aptamer protons |
|---|---|
| H4 | T4-H3<br>G28-H1<br>A30-H2 |
| H9 | T4-Me, H6 |
| H14 | G28-H8 |
| H12 | G28-H2'/2'', H8 |
| H21 | C29-H6, H5, H2'/2'', H3'<br>C5-H41<br>T15-H1', H4'<br>A30-H1', H4', H8, H2<br>T4-H3<br>G28-H1 |
| H16/20 | G28-H2'/2'', H3', H8 |
| H17/19 | G28-H2'/2'', H3', H8<br>A27- H2'/2'', H3' |
| H18 | G28-H2'/2'', H3', H8<br>A27- H2'/2'', H3' |

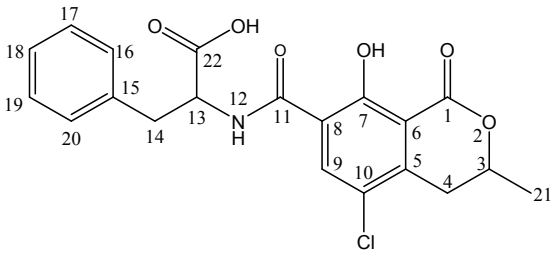


OTA structure

**Table S5**. Intermolecular NOEs between OTB and OBA33 aptamer protons in OBA33-OTB complex.

| **OTB protons** | **OBA33 aptamer protons** |
|---|---|
| H4 | T4-H3<br>G28-H1<br>A30-H2 |
| H9 | T4-Me, H6 |
| H10 | T4-Me |
| H12 | G28-H2'/2'', H8 |
| H21 | C29-H6, H5, H2'/2'', H3'<br>C5-H41<br>T15-H1', H4'<br>A30-H1', H4', H8, H2<br>T4-H3<br>G28-H1 |
| H16/20 | G28-H2'/2'', H3', H8 |
| H17/19 | G28-H2'/2'', H3', H8<br>A27- H2'/2'', H3' |
| H18 | G28-H2'/2'', H3', H8<br>A27- H2'/2'', H3' |

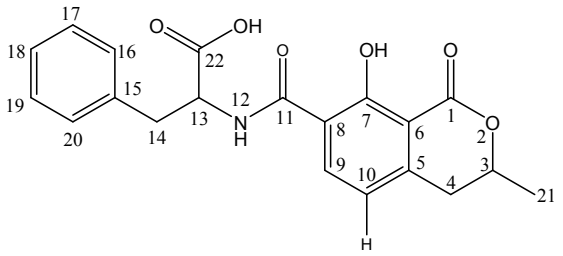


OTB structure

**Table S6.** OBA32 aptamer and its inosine-substituted variants sequences.

| Name | Sequence (5'→3') |
|---|---|
| OBA32 | GATCGGGTGTGGGTGGCGTAAAGGGAGCATCG |
| OBA32-I2 | **I** ATCGGGTGTGGGTGGCGTAAAGGGAGCATCG |
| OBA32-I6 | GATC**I** GGTGTGGGTGGCGTAAAGGGAGCATCG |
| OBA32-I8 | GATCGG**I** TGTGGGTGGCGTAAAGGGAGCATCG |
| OBA32-I10 | GATCGGGT**I** TGGGTGGCGTAAAGGGAGCATCG |
| OBA32-I12 | GATCGGGTGT**I** GGTGGCGTAAAGGGAGCATCG |
| OBA32-I16 | GATCGGGTGTGGGT**I** GCGTAAAGGGAGCATCG |
| OBA32-I17 | GATCGGGTGTGGGTG**I** CGTAAAGGGAGCATCG |
| OBA32-I24 | GATCGGGTGTGGGTGGCGTAAA**I** GGAGCATCG |
| OBA32-I26 | GATCGGGTGTGGGTGGCGTAAAGG**I** AGCATCG |
| OBA32-I28 | GATCGGGTGTGGGTGGCGTAAAGGGA**I** CATCG |